

Ion mobility studies on the negative ion-molecule chemistry of pentachloroethane

González-Méndez, R, Watts, P, Howse, DC, Procino, I, McIntyre, H & Mayhew, CA

Author post-print (accepted) deposited by Coventry University's Repository

Original citation & hyperlink:

González-Méndez, R, Watts, P, Howse, DC, Procino, I, McIntyre, H & Mayhew, CA 2017, 'Ion mobility studies on the negative ion-molecule chemistry of pentachloroethane' *International Journal of Mass Spectrometry*, vol 417, pp. 16-21 <https://dx.doi.org/10.1016/j.ijms.2017.04.011>

DOI 10.1016/j.ijms.2017.04.011

ISSN 1387-3806

Publisher: Elsevier

NOTICE: this is the author's version of a work that was accepted for publication in *International Journal of Mass Spectrometry*. Changes resulting from the publishing process, such as peer review, editing, corrections, structural formatting, and other quality control mechanisms may not be reflected in this document. Changes may have been made to this work since it was submitted for publication. A definitive version was subsequently published in *International Journal of Mass Spectrometry*, [417, (2017)] DOI: 10.1016/j.ijms.2017.04.011

© 2017, Elsevier. Licensed under the Creative Commons Attribution-NonCommercial-NoDerivatives 4.0 International

<http://creativecommons.org/licenses/by-nc-nd/4.0/>

Copyright © and Moral Rights are retained by the author(s) and/ or other copyright owners. A copy can be downloaded for personal non-commercial research or study, without prior permission or charge. This item cannot be reproduced or quoted extensively from without first obtaining permission in writing from the copyright holder(s). The content must not be changed in any way or sold commercially in any format or medium without the formal permission of the copyright holders.

This document is the author's post-print version, incorporating any revisions agreed during the peer-review process. Some differences between the published version and this version may remain and you are advised to consult the published version if you wish to cite from it.

1 **ION MOBILITY STUDIES ON THE NEGATIVE ION-MOLECULE**
2 **CHEMISTRY OF PENTACHLOROETHANE**

3 Ramón González-Méndez,^{1*} Peter Watts,¹ David C. Howse,¹ Immacolata Procino,² Henry
4 McIntyre,² and Chris A. Mayhew^{1,3}

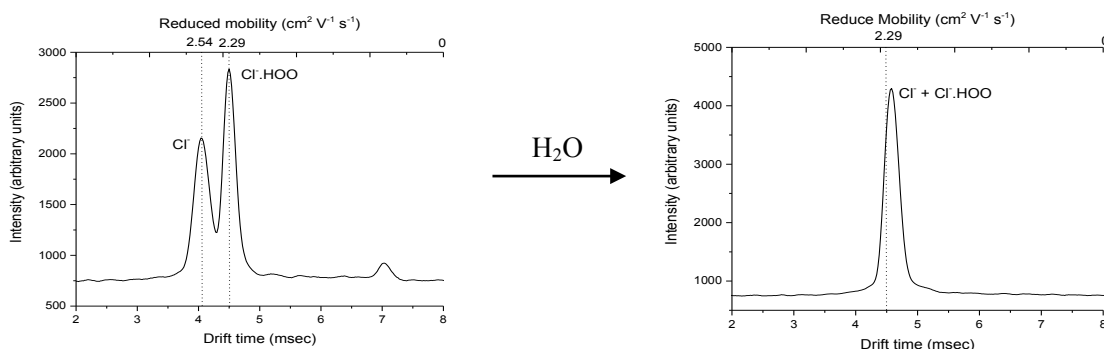
- 5 1. School of Physics and Astronomy, University of Birmingham, Edgbaston,
6 Birmingham, B15 2TT, UK
7 2. Smiths Detection, Century House, Maylands Avenue, Hemel Hempstead,
8 Hertfordshire, HP2 7DE, UK
9 3. Institut für Atemgasanalytik, Leopold-Franzens-Universität Innsbruck, Rathausplatz
10 4, A-6850 Dornbirn, Austria
11

12 * Corresponding Author Tel.:+44 121 414 4668. E-mail: R.GonzalezMendez@bham.ac.uk

13
14 Key words: Ion Mobility Spectrometry; IMS-MS; Pentachloroethane; Chlorinated Ethane;
15 Ion-Molecule Chemistry

16
17 **GRAPHICAL ABSTRACT**

18



19

20 **Abstract**

21 In this study we present an investigation of the negative ion-molecule chemistry of
22 pentachloroethane (PCE) in air based Ion Mobility Spectrometry and Ion Mobility
23 Spectrometry-Mass Spectrometry systems. The observed product ions are Cl^- , produced by
24 dissociative electron attachment, and $\text{Cl}^- \cdot \text{HOO}$ resulting from a reaction with O_2^- . Based upon
25 the moisture content of the system, these ions can be observed as a doublet in a 'dry' system
26 or as a singlet in a 'wet' system. The nature of the $\text{Cl}^- \cdot \text{HOO}$ product ion was investigated by
27 using isoflurane (ISOF) as a probe to monitor the changing ratios of Cl^- and $\text{Cl}^- \cdot \text{HOO}$ as the
28 PCE concentration decreased. This confirmed the origins of the two product anions.
29 Electronic structure calculations are provided. These have aided the understanding of the
30 reaction processes observed.

31

32

33 **1. Introduction**

34 The ability to quickly and accurately identify hazardous compounds, and particularly within a
35 complex chemical environment, is vital to homeland security. Ion Mobility Spectrometry
36 (IMS) has found worldwide deployment in security areas such as airports. However, it has
37 limitations in terms of selectivity, and false positives do occur. To limit these, the ion
38 chemistry in the reaction of the region of the IMS can be manipulated. This is achieved by
39 doping the carrier gas. Chlorine containing compounds are used in ion mobility spectrometers
40 operating in negative ion mode to enhance specificity and sensitivity.¹⁻¹² Unfortunately the
41 most suitable, in terms of its facile dissociative electron attachment (DEA) with thermal
42 electrons and its volatility, is carbon tetrachloride, CCl₄, which is now banned by the
43 Montreal Protocol.¹³ Hexachloroethane, HCE, is commonly used in laboratory investigations,
44 and has been described in a recent paper on the ion-molecule chemistry of the anaesthetics
45 isoflurane (ISOF, CF₃CHClOCHF₂) and enflurane (ENF, CHF₂OCF₂CHFCl).¹⁴ However, its
46 vapour pressure at low temperatures makes it unsuitable for use in practical systems for use
47 in the field. The volatility of pentachloroethane, PCE (CCl₃CHCl₂), makes it more suitable
48 for use in such practical devices as the Smiths Detection Lightweight Chemical Detector used
49 in this study.¹⁵

50 The investigation presented in this paper continues our work on the negative ion-
51 molecule chemistry of chlorinated compounds in IMS systems.¹⁴ Two systems have been
52 used for this work, a Smiths Detection IMS - henceforth referred to as the Smiths system,¹⁵
53 and a home-made IMS/MS located in the Molecular Physics Group at the University of
54 Birmingham - referred to as the Birmingham system. An additional motivation for this study
55 comes from preliminary experiments with PCE, which in the Birmingham IMS/MS system
56 showed only one ion mobility peak, whilst the Smiths IMS system showed a doublet peak
57 structure. The results of the present study, which used ISOF as a probe compound, allowed
58 these apparently conflicting observations to be rationalised.

59 The experimental work presented in this paper is supported by electronic structure
60 calculations at the B3LYP level, which provide useful energetic calculations for the DEA
61 processes and various chemical reactions.

62

63 **2. Experimental Details**

64 **2.1. Ion Mobility Spectrometry (IMS) and Ion Mobility Spectrometry-Mass** 65 **Spectrometry (IMS/MS)**

66 The Birmingham IMS/MS system used in this study has been described elsewhere,¹⁶⁻
67 ²⁰ and hence only a brief description is provided here. This instrument consists of two glass
68 drift tube regions each of 10 cm in length. The first, the reaction region containing a
69 cylindrical radioactive ion source (nominal 10 mCi ⁶³Ni foil), is physically separated from the
70 second region, the drift region, by a Bradbury-Nielson (B-N) gate. A forward flow of the
71 buffer gas flows through the radioactive source and into the glass jacket towards the B-N
72 grid. A contraflow of the same buffer gas is introduced through apertures near to a Faraday
73 plate (FP). The analyte of interest is introduced in the forward flow with the help of syringes.
74 Forward and contraflows are set at 0.4 L min⁻¹ and 0.8 L min⁻¹ (at slightly above the ambient
75 atmospheric pressure and room temperature), respectively, and controlled by mass flow
76 controllers (Alicat Scientific, Arizona, USA, ±1% accuracy). The two flows are vented out of
77 the drift tube through holes in the B-N ring. The drift tube's pressure is measured with a
78 strain gauge absolute pressure sensor (Edwards, West Sussex, UK, model ASG 2000). A
79 thermocouple is used to monitor the temperature of the buffer gas near to the exhaust region
80 and the temperature of the drift tube is electronically controlled at a constant temperature of
81 30 ± 1°C. An electric field along the axis of the drift tube is set at 200 V cm⁻¹.

82 The FP is protected by a screen grid to shield it from the electric field produced by the
83 oncoming ion swarm. At the centre of the FP there is a 0.07 mm pinhole, separating the IMS
84 from the lower pressure quadrupole mass spectrometer region. The product ions are separated
85 according to their m/z values using quadrupole mass filter and detected using a secondary
86 electron multiplier. For this identification of the m/z values the B-N grid in the drift tube is
87 kept open in order to maximise ion signal intensity.

88 To obtain ion mobility spectra, the B-N gate is used to pulse reactant and product ions
89 generated in the reaction region into the drift region tube at a frequency of 25 Hz and a pulse
90 width of 600 μs (600 μs was necessary, because at shorter pulse widths the ion signals
91 associated with isoflurane and enflurane were significantly weaker, presumably owing to the
92 transit times of the product ions through the B-N grid). Mobility spectra were acquired by
93 means of purposely written software using Labview.²⁰ Total ion mobility spectra were
94 acquired using the FP. Tuned ion mobility spectra were obtained by sampling ions through
95 the FP and then allowing a specific m/z through the mass filter. The tuned ion mobility
96 spectra were used to verify contributions of product ions to the individual peaks in the total
97 ion mobility spectra.²⁰

98 The Smiths system used is a modified Lightweight Chemical Detector (LCD).^{15,21}
99 Two IMS cells, one for positive ions and one for negative ions, are housed in the same

100 instrument. The data presented in this paper were acquired in the negative mode cell. Each
101 cell consists of two regions: reaction and drift regions. The reaction region, containing a dual-
102 point corona discharge ionization source,²² is open to ambient air via a pinhole through which
103 air is pulled into the system for sampling. Connected to the reaction region are On-demand
104 Vapour Generators (OVGs) for injecting PCE and isoflurane in the system.²³ The ions
105 generated in the reaction region migrate under the influence of an electric field towards a B-N
106 gate. Once transferred through the B-N gate in the drift region, the ions drift towards a FP for
107 detection. The electric field, generated by applying a voltage gradient across the electrodes
108 placed along the whole drift tube length (reaction and drift regions), was set to be about 200
109 V cm⁻¹. The drift gas has a flow of 150 mL min⁻¹ and consists of air at atmospheric pressure.
110 It is generated by a fan which recirculates air through the IMS cells and a molecular sieve.
111 The molecular sieve traps water in order to keep a low level of moisture in the system. In
112 order to increase the moisture level in the IMS cell, a fraction of the drift gas was pumped
113 from the body of molecular sieve, circulated in the headspace above a saturated solution of
114 lithium chloride (headspace air with relative humidity of 11.30%), and mixed back into the
115 drift air flow close to the FP.

116

117 **2.2 Procedures and chemicals**

118 Isoflurane (with stated purity of 99%) was purchased from Sigma Aldrich (Dorset, UK).
119 Pentachloroethane (96% pure) was purchased from Alfa Aesar (Lancashire, UK). All the
120 samples were used without further purification. At room temperature they are both liquids.

121 In the Birmingham system, typically 50 μ L were spotted onto cotton and placed
122 inside a glass syringe (Weber Scientific, New Jersey, USA) which was inserted through a
123 septum into the forward flow at a constant rate using a syringe driver (Cole Palmer 74900
124 series, Illinois, USA). In the Smiths system, OVGs were used as the sampling method.

125 Zero air grade and pure nitrogen (oxygen free and 99.998% purity) carrier gases used
126 for this experiment were purchased from BOC Gases (Manchester, UK). Prior to entering the
127 reaction region all carrier gases were passed through moisture and hydrocarbon traps
128 (Supelco 23991 and Agilent BHT-4 respectively).

129

130 **2.3. Density Functional Theory (DFT) Calculations**

131 These were conducted using Gaussian09W and GaussView05 for Windows.²⁴ Unless
132 otherwise stated all calculations used the B3LYP functional and the 6-31+G(d,p) basis set, a
133 combination which has been found to be satisfactory.¹⁴ Stable species were characterised by

134 the absence of an imaginary frequency. Vertical Attachment Energies (VAEs) were
135 determined by doing a frequency job after placing a negative charge on the ground state
136 geometry of the neutral.

137

138 3. Results and Discussion

139 3.1 Pentachloroethane

140

141 3.1.1 Electron attachment

142 DEA in nitrogen to give both Cl^- and Cl_2^- is thermodynamically favourable (Table 1)
143 although only the former is observed.

144

145 Table 1. Calculated ΔH s and ΔG s for the DEA of PCE leading to Cl^- and Cl_2^- . DFT
146 calculations were performed using the B3LYP functional and the 6-31+G(d,p) basis set.

Reactants	Ionic products	$\Delta\text{H}_{298} \text{ kJ mol}^{-1}$	$\Delta\text{G}_{298} \text{ kJ mol}^{-1}$
PCE + e	Cl^-	-119	-161
	Cl_2^-	-190	-244

147

148 The calculated VAE is negative (-7.0 kJ mol^{-1}) as expected from the observed
149 resonance with electrons at 0 eV. No Cl_2^- was observed, although it is reported to occur at 0
150 eV by Matias *et al* in a study involving DEA at low pressures.²⁵

151

152 3.1.2 Reactions in air

153 In the Birmingham system only a single IMS peak was observed. Tuned m/z experiments
154 showed it to be a mixture of $\text{Cl}^-(\text{H}_2\text{O})_n$ ($n=0,1$) and m/z 68. Figure 1 shows the Reactant Ion
155 Peak (RIP) for (a) air (b) for PCE (obtained in the system sufficiently doped with PCE for the
156 air RIP to be fully depleted).

157

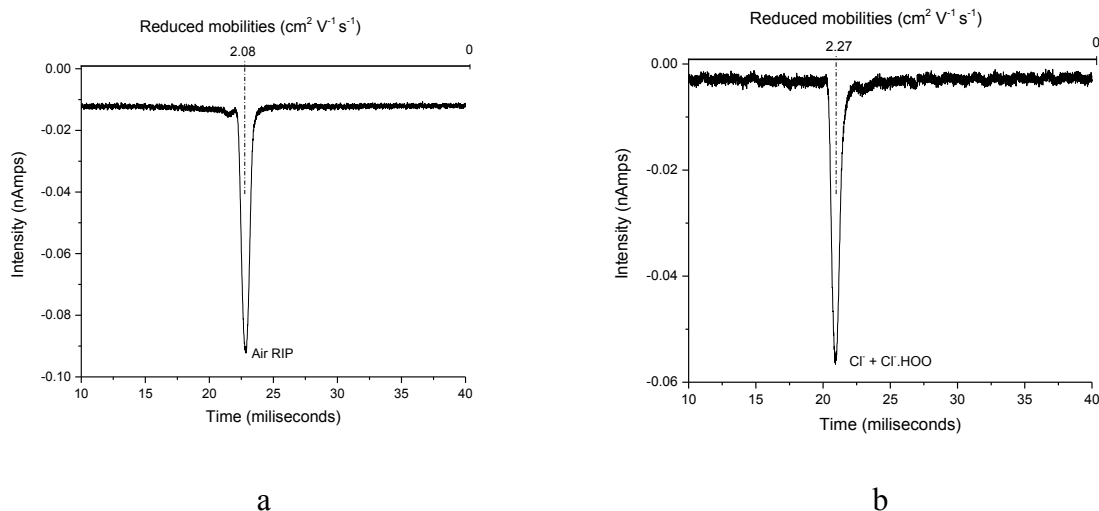


Figure 1. IMS spectra showing the RIP for (a) an air system and (b) for a heavily doped PCE system. In all figures only the core ions are given in the annotations, water clusters have been omitted.

158

159 As the concentration of PCE reduced, but with the air RIP still completely depleted, a
 160 peak on the low mobility side of the PCE RIP appeared (figure 2). Tuned ion mobility
 161 showed that this results from an anion at m/z 68. This is ascribed to be $\text{Cl}^{\cdot}\text{HOO}$ (see later).

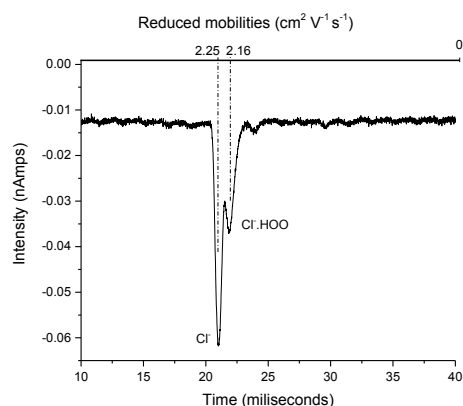


Figure 2. IMS spectrum in an air system doped with PCE at a lower concentration of PCE than in figure 1 (b), but still sufficiently high to completely deplete the air RIP.

162

163 In the Smiths system (see Figures 3a and 3b), under very dry conditions (it is not
 164 possible to be quantitative at such low water concentrations in such a small IMS device)
 165 either a singlet or a doublet or various intermediate mobility peaks could be observed
 166 dependent upon the PCE and water concentrations. In Figures 3a and 3b the more mobile
 167 peaks are ascribed to Cl^{\cdot} and the less mobile peaks to $\text{Cl}^{\cdot}\text{HOO}$. Figure 3a shows that as the
 168 humidity increases the Cl^{\cdot} peak decreases in mobility due to hydration subsequently merging

169 with the Cl⁻.HOO. As will be seen later, Cl⁻ readily complexes with one H₂O molecule,
 170 whereas Cl⁻.HOO does not. Figure 3b shows that as the PCE concentration increases the ratio
 171 Cl⁻.HOO to Cl⁻ decreases.

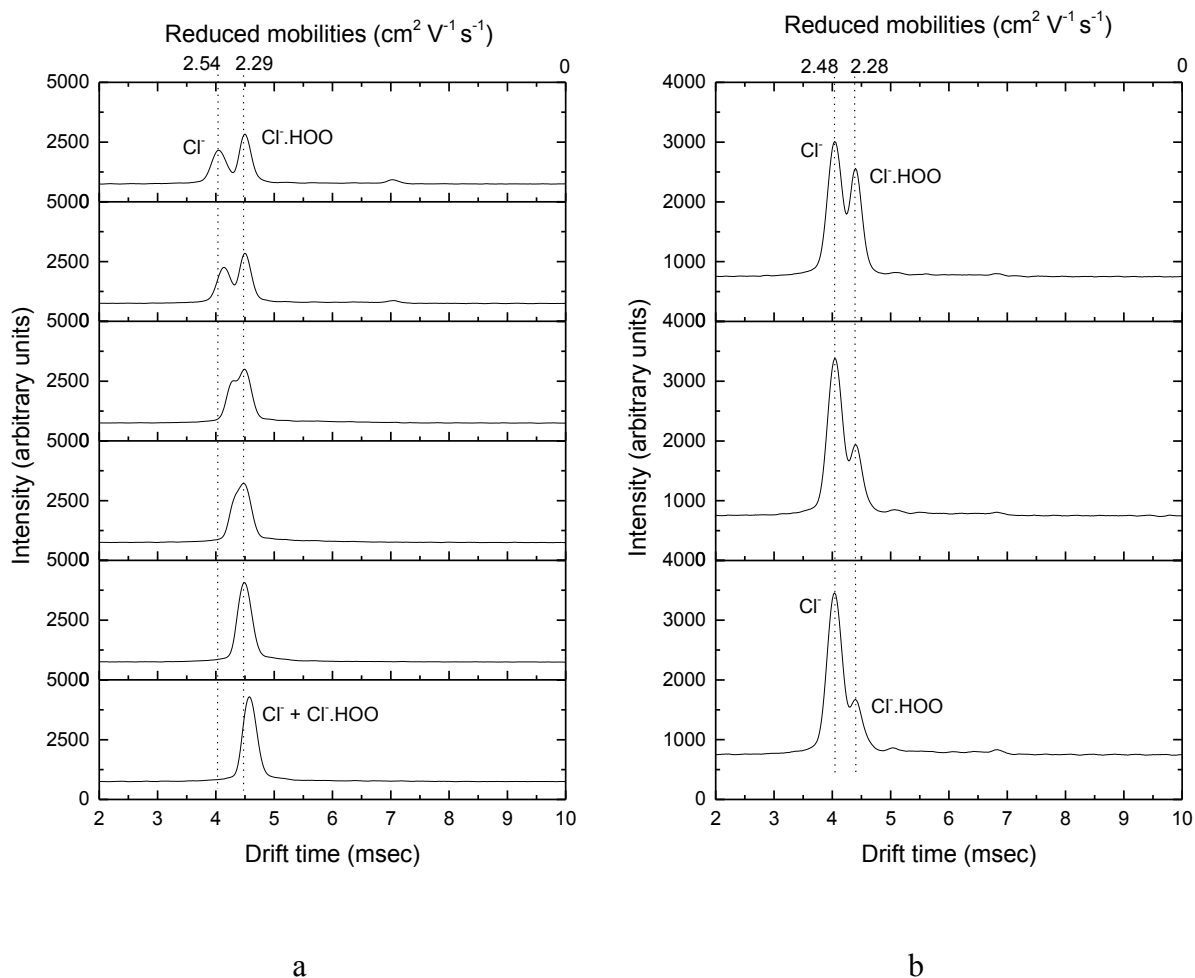


Figure 3. (a) IMS spectra of PCE showing the effect of the internal moisture and how, as the humidity increases, the Cl⁻ peak decreases in mobility due to hydration subsequently merging with the Cl⁻.HOO peak. The level of moisture gradually increases from the top to the bottom plot. (b) IMS spectra of PCE acquired at different PCE concentrations showing the effect of the PCE concentration on the relative intensities of Cl⁻ and Cl⁻.HOO. The PCE concentration gradually increases from the top to the bottom plot.

172

173 A detailed inspection of the results showed that, dependent upon the PCE and water
 174 concentrations, either a singlet or a doublet or various intermediate mobility peaks could be
 175 observed both in the Smiths and Birmingham systems.

176

177 The ion with m/z 68 is assigned as $\text{Cl}^-\cdot\text{HOO}$ as DFT calculations showed that it is
178 essentially Cl^- hydrogen bonded to HOO (figure 4).

179

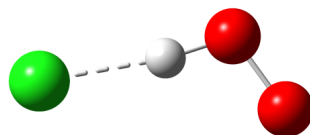


Figure 4. Structure of $\text{Cl}^-\cdot\text{HOO}$ obtained from DFT calculations.

180

181 The same result is obtained starting from Cl^- associating with OOH as from HCl
182 associating with O_2^- . As electron attachment to PCE in the IMS system gives only Cl^- , it can
183 be safely assumed that the formation of $\text{Cl}^-\cdot\text{HOO}$ arises from the reaction of PCE with O_2^- .
184 The overall energetics for this reaction are $\Delta H_{298} -180 \text{ kJ mol}^{-1}$ and $\Delta G_{298} -196 \text{ kJ mol}^{-1}$,
185 assuming that the neutral product is CCl_2CCl_2 . This is supported by the observation that as
186 the concentration of PCE increased so did the proportion of Cl^- as would be expected if O_2^-
187 and PCE are in competition for the electrons. The initial (albeit transient) product of the
188 reaction of O_2^- with PCE is a complex with the oxygen close to the hydrogen of the PCE, as
189 shown in Figure 5, and Table 2 for the energetics. An alternative conformation with the
190 oxygen orientated away from the CCl_3 group is slightly less stable.

191

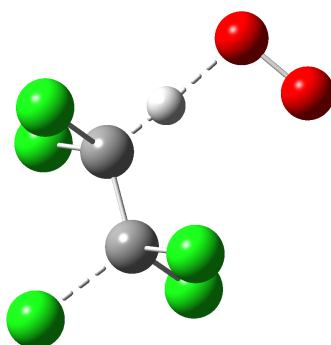


Figure 5. Structure of $\text{PCE}\cdot\text{O}_2^-$ complex obtained from DFT calculations.

192

193

194

195

196

197 Table 2. Energetics for the formation of various species relative to PCE + O₂⁻. DFT
 198 calculations were performed using the B3LYP functional and the 6-31+G(d,p) basis set.

Reaction	Species	ΔH_{298} kJ mol ⁻¹	ΔG_{298} kJ mol ⁻¹
1	Complex PCE.O ₂ ⁻ (Fig 4)	-104	-73
2	C ₂ Cl ₅ ⁻ + HOO	-82	-107
3	C ₂ Cl ₄ + Cl ⁻ + HOO	-70	-113
4	C ₂ Cl ₄ + Cl ⁻ .HOO	-180	-196
5	CHCl ₂ CCl ₂ + Cl ⁻ + O ₂	-59	-102
6	Barrier for rotation around the C-C bond of PCE	+38	+43
7	Barrier for rotation around the C-C bond of PCE.O ₂ ⁻	+33	+22

199
 200 Of primary interest is the formation of Cl⁻.HOO. Reactions 3 and 5 may contribute to
 201 the production of Cl⁻ but are probably of little importance compared to the DEA with free
 202 electrons. It is not proposed that reactions 2 and 3 occur (except as precursors to reaction 4)
 203 but are included to illustrate that sufficient energy is available in the transient PCE.O₂⁻
 204 complex to allow complex conformational changes to occur. This is necessary as formation
 205 of Cl⁻.HOO from the complex (reaction 4) requires a concerted lengthening on the C-H bond
 206 and a rotation of the C-Cl bonds around the C-C bond. Despite many attempts no transition
 207 state has yet been found, and this difficulty is attributed to the proposed concerted nature of
 208 the transition state.

209 210 3.1.3 Reactions of H₂O with Cl⁻ and Cl⁻.HOO

211 It can be seen from Table 3 that Cl⁻ will readily complex with one water, but that Cl⁻.HOO
 212 will not as the HOO is effectively solvating Cl⁻, i.e. taking the place of H₂O in the Cl⁻.H₂O
 213 complex. The strength of the Cl⁻.HOO complex can be seen in the last row of Table 3. Thus
 214 in a 'dry' system the doublet of Cl⁻ and Cl⁻.HOO is observed and as the water concentration
 215 increases the Cl⁻ complexes with water thus decreasing its mobility and eventually merging
 216 with the Cl⁻.HOO to give a singlet (see Figure 1b).

217

218 Table 3. Calculated ΔH s and ΔG s for the reactions of $\text{Cl}^{\cdot}(\text{H}_2\text{O})_n$ ($n = 0, 1$ and 2) with H_2O ,
 219 Cl^{\cdot} with HOO^{\cdot} , and $\text{Cl}^{\cdot}.\text{HOO}(\text{H}_2\text{O})_n$ ($n = 0$ and 1) with H_2O . DFT calculations performed
 220 using the B3LYP functional and the 6-31+G(d,p) basis set.

Reactants	Products	$\Delta H_{298} \text{ kJ mol}^{-1}$	$\Delta G_{298} \text{ kJ mol}^{-1}$
$\text{Cl}^{\cdot} + \text{H}_2\text{O}$	$\text{Cl}^{\cdot}.\text{H}_2\text{O}$	-60	-37
$\text{Cl}^{\cdot}.\text{H}_2\text{O} + \text{H}_2\text{O}$	$\text{Cl}^{\cdot}.\text{2H}_2\text{O}$	-54	-18
$\text{Cl}^{\cdot}.\text{2H}_2\text{O} + \text{H}_2\text{O}$	$\text{Cl}^{\cdot}.\text{3H}_2\text{O}$	-47	-10
$\text{Cl}^{\cdot}.\text{HOO} + \text{H}_2\text{O}$	$\text{Cl}^{\cdot}.\text{HOO}.\text{H}_2\text{O}$	-52	-16
$\text{Cl}^{\cdot}.\text{HOO}.\text{H}_2\text{O} + \text{H}_2\text{O}$	$\text{Cl}^{\cdot}.\text{HOO}.\text{2H}_2\text{O}$	-44	-7
$\text{Cl}^{\cdot} + \text{HOO}^{\cdot}$	$\text{Cl}^{\cdot}.\text{HOO}^{\cdot}$	-111	-83

221

222 3.2 Reaction of ISOF in a PCE doped system

223 As a way to fully understand the occurring chemistry, the properties of the $\text{Cl}^{\cdot}.\text{HOO}$ ion were
 224 investigated by using ISOF as a probe in both instruments. For such a purpose sufficient PCE
 225 was introduced to replace the air RIP (figure 1a) with a PCE RIP of Cl^{\cdot} and $\text{Cl}^{\cdot}.\text{HOO}$ (figure
 226 1b). In the Birmingham system, addition of ISOF (shown in Figure 6a) results in the
 227 formation of two product ions m/z analysed as $\text{ISOF}.\text{Cl}^{\cdot}$ and $\text{ISOF}.\text{Cl}^{\cdot}.\text{HOO}$ the latter being
 228 the less mobile peak. The IMS spectrum in Figure 6b (when compared with that shown in
 229 figure 6a) demonstrates the variability in relative proportions of product ions. For figure 6b
 230 the PCE concentration had been allowed to decay as can be seen by the appearance of the air
 231 RIP at reduced mobility $K_0 = 2.08 \text{ cm}^2 \text{ V}^{-1} \text{ s}^{-1}$. In Section 3.1.2 it was suggested that as the
 232 PCE concentration decreased the ratio of $\text{Cl}^{\cdot}.\text{HOO}/\text{Cl}^{\cdot}$ would increase, and this is well
 233 demonstrated by the changing ratios of $\text{ISOF}.\text{Cl}^{\cdot}$ and $\text{ISOF}.\text{Cl}^{\cdot}.\text{HOO}$ in Figures 6a and 6b.

234

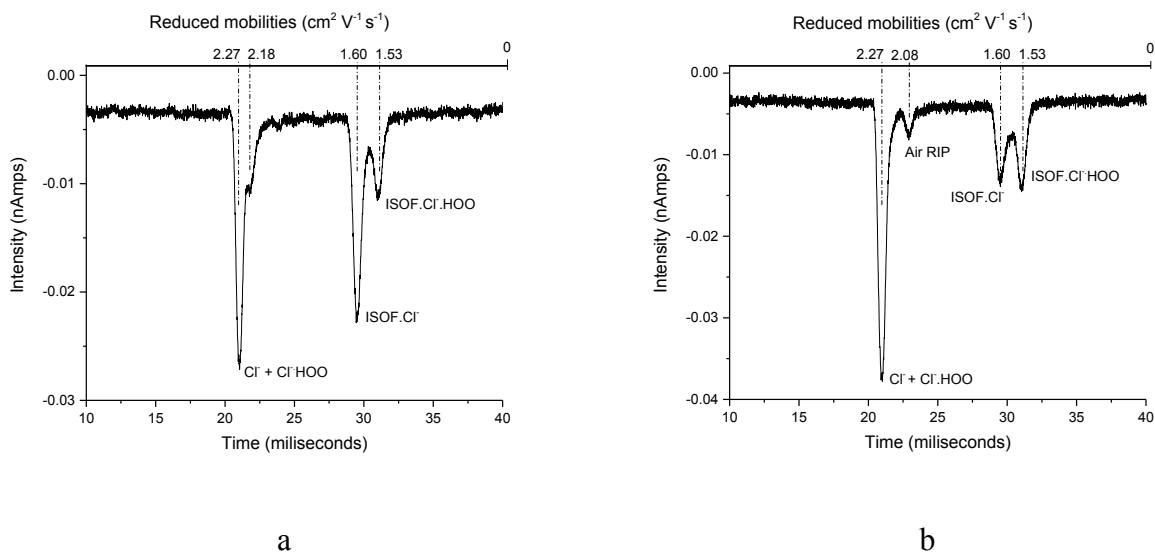


Figure 6. (a) IMS spectrum for an air system doped with PCE with ISOF added. (b) IMS spectrum for an air system doped with PCE (in lower concentration when compared with 6a) following addition of ISOF. The small peak at $K_0 = 2.08 \text{ cm}^2 \text{V}^{-1} \text{s}^{-1}$ is the remnant of the air RIP.

235

236 For the Smiths system results of similar experiments are shown in figure 7 under wet
 237 and dry conditions.

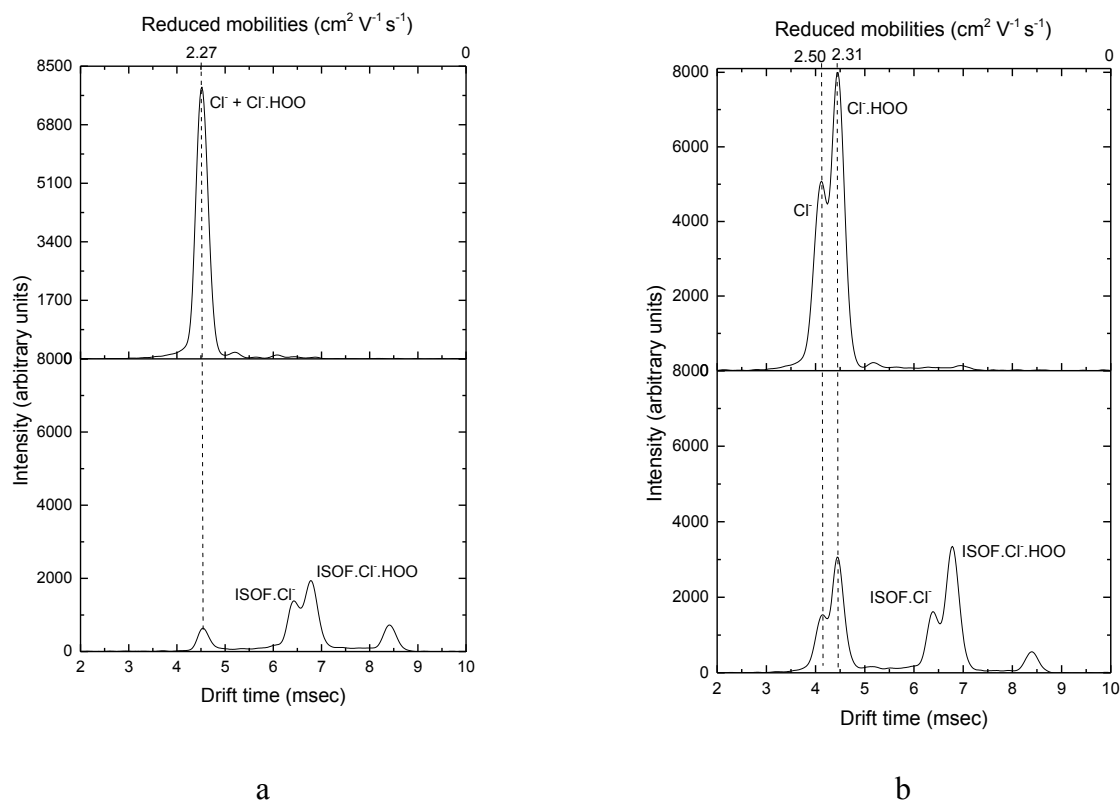


Figure 7. Smiths IMS spectra of PCE (top line plots) and ISOF (bottom line plots) acquired in a PCE doped system in a) “wet” conditions; b) “dry” conditions.

238 DFT calculations provided stable structures for the ISOF.Cl⁻.HOO and ISOF.Cl⁻
 239 product ions, as shown in Figure 8.

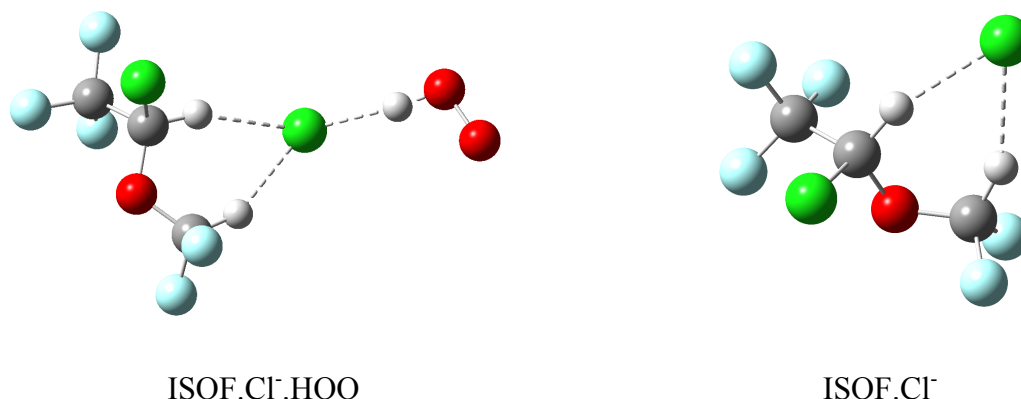


Figure 8. Structure of ISOF monomer product ions ISOF.Cl⁻.HOO and ISOF.Cl⁻ obtained from DFT calculations.

240
 241 The energetics for the reactions of ISOF with Cl⁻ and Cl⁻.HOO are summarised in
 242 Table 4.

243
 244 Table 4. ΔHs and ΔGs for the reaction of ISOF with various anions. DFT calculations
 245 performed using the B3LYP functional and the 6-31+G(d,p) basis set.

Reactants	Ionic Products	ΔH ₂₉₈ kJ mol ⁻¹	ΔG ₂₉₈ kJ mol ⁻¹
ISOF + Cl ⁻ .HOO	ISOF.Cl ⁻ .HOO	-76	-50
ISOF.Cl ⁻ .HOO + ISOF	ISOF ₂ .Cl ⁻ .HOO	-58	-2
ISOF + Cl ⁻	ISOF.Cl ⁻	-108	-79
ISOF.Cl ⁻ + ISOF	ISOF ₂ .Cl ⁻	-74	-40

246
 247 Calculations showed that the dimer complex of ISOF and Cl⁻.HOO is thermo neutral
 248 and even if formed it will be unstable in the drift region and hence is unlikely to be observed
 249 in accord with experiment.

250
 251 **4. Conclusions**

252 After introduction of PCE into an air based IMS system, two product ions were observed, Cl⁻
 253 by DEA and Cl⁻.HOO by reaction with O₂⁻. These anions can be observed as a doublet in a
 254 ‘dry’ system or as a singlet in a ‘wet’ system. In the wet system Cl⁻ clusters with water thus
 255 reducing its mobility whereas Cl⁻.HOO does not. Because DEA and reaction with O₂⁻ are in
 256 competition the ratio of the two product ions is dependent upon PCE concentration. An

257 additional factor leading to this dependence is that PCE and O₂ are competing for electrons,
258 the PCE leading to Cl⁻ through DEA and the O₂ leading to O₂⁻. Cl⁻.HOO complexes with
259 ISOF as does Cl⁻. This is nicely demonstrated by two ISOF product peaks being observed
260 even in a wet system when only a singlet PCE based RIP is observed.

261 The results presented here illustrate the care that must be taken in interpreting even
262 apparently simple chemical systems in an IMS instrument. Electronic structure calculations
263 have provided valuable insight into the processes observed.

264

265 **Acknowledgements**

266 The Early Stage Researcher (RGM) acknowledges the support of the PIMMS Initial Training
267 Network which in turn is supported by the European Commission's 7th Framework
268 Programme under Grant Agreement Number 287382.

269

270 **References**

271 1. Puton, J.; Nousiainen, M.; Sillanpää, M., Ion mobility spectrometers with doped
272 gases. *Talanta* **2008**, *76* (5), 978-987.

273 2. Ewing, R. G.; Atkinson, D. A.; Eiceman, G. A.; Ewing, G. J., A critical review of ion
274 mobility spectrometry for the detection of explosives and explosive related compounds.
275 *Talanta* **2001**, *54* (3), 515-529.

276 3. Spangler, G. E.; Carrico, J. P.; Campbell, D. N., Recent advances in ion mobility
277 spectrometry for explosives vapor detection. *Journal of Testing and Evaluation* **1985**, *13* (3),
278 234-240.

279 4. Daum, K. A.; Atkinson, D. A.; Ewing, R. G., Formation of halide reactant ions and
280 effects of excess reagent chemical on the ionization of TNT in ion mobility spectrometry.
281 *Talanta* **2001**, *55* (3), 491-500.

282 5. Proctor, C. J.; Todd, J. F. J., Alternative reagent ions for plasma chromatography.
283 *Analytical Chemistry* **1984**, *56* (11), 1794-1797.

284 6. Rajapakse, M. Y.; Stone, J. A.; Eiceman, G. A., Decomposition Kinetics of
285 Nitroglycerine·Cl⁻(g) in Air at Ambient Pressure with a Tandem Ion Mobility Spectrometer.
286 *The Journal of Physical Chemistry A* **2014**, *118* (15), 2683-2692.

287 7. Rajapakse, R. M. M. Y.; Stone, J. A.; Eiceman, G. A., An ion mobility and theoretical
288 study of the thermal decomposition of the adduct formed between ethylene glycol dinitrate
289 and chloride. *International Journal of Mass Spectrometry* **2014**, *371* (0), 28-35.

- 290 8. Kozole, J.; Levine, L. A.; Tomlinson-Phillips, J.; Stairs, J. R., Gas phase ion
291 chemistry of an ion mobility spectrometry based explosive trace detector elucidated by
292 tandem mass spectrometry. *Talanta* **2015**, *140* (0), 10-19.
- 293 9. Li, G.; Zhang, Z.; Huang, Q.; Guo, T.; Zhang, X., A Novel Pulsed Doping Method for
294 Enhancing the Sensitivity of Ion Mobility Spectrum (IMS) for Detecting Explosives and a
295 Mechanism Study. *Sensor Letters* **2015**, *13* (9), 778-784.
- 296 10. Lawrence, A. H.; Neudorfl, P., Detection of ethylene glycol dinitrate vapors by ion
297 mobility spectrometry using chloride reagent ions. *Analytical Chemistry* **1988**, *60* (2), 104-
298 109.
- 299 11. Matz, L. M.; Tornatore, P. S.; Hill, H. H., Evaluation of suspected interferents for
300 TNT detection by ion mobility spectrometry. *Talanta* **2001**, *54* (1), 171-179.
- 301 12. Ewing, R.; Atkinson, D.; Benson, M., Atmospheric pressure ionization of chlorinated
302 ethanes in ion mobility spectrometry and mass spectrometry. *Int. J. Ion Mobil. Spec.* **2015**, *18*
303 (1-2), 51-58.
- 304 13. Montreal Protocol on Substances that Deplete the Ozone Layer. 1522 UNTS 3; 26
305 ILM 1550 (1987). <http://www.unep.org/OZONE/pdfs/Montreal-Protocol2000.pdf> (accessed
306 29-03-2017)
- 307 14. González-Méndez, R.; Watts, P.; Howse, D.C.; Procino, I.; McIntyre, H.; Mayhew C.
308 A, Ion mobility studies on the negative ion-molecule chemistry of isoflurane and enflurane.
309 *Journal of the American Society for Mass Spectrometry*. **2017**, Feb 21 (DOI:[10.1007/s13361-](https://doi.org/10.1007/s13361-017-1616-0)
310 [017-1616-0](https://doi.org/10.1007/s13361-017-1616-0) . [Epub ahead of print]).
- 311 15. Detection, S. High Performance CWA Identifier And TIC Detector.
312 [http://www.smithsdetection.com/index.php?option=com_k2&view=item&id=86&Itemid=60](http://www.smithsdetection.com/index.php?option=com_k2&view=item&id=86&Itemid=600#.WAi4JHoVqzs)
313 [0#.WAi4JHoVqzs](http://www.smithsdetection.com/index.php?option=com_k2&view=item&id=86&Itemid=600#.WAi4JHoVqzs) (accessed 29-03-2017).
- 314 16. Liu, Y., Mayhew, C.A. and Peverall, R., A new experimental approach to investigate
315 the kinetics of low energy electron attachment reactions. *International journal of mass*
316 *spectrometry and ion processes* **1996**, *152*(2), 225-242.
- 317 17. Jarvis, G. K., Peverall, R. and Mayhew, C. A., A novel use of an ion-mobility mass
318 spectrometer for the investigation of electron attachment to molecules. *Journal of Physics B:*
319 *Atomic, Molecular and Optical Physics* **1996**, *29*(19) L713.
- 320 18. Jarvis, G. K., Mayhew, C. A., Singleton, L., and Spyrou, S. M. An investigation of
321 electron attachment to CHCl₂F, CHClF₂ and CHF₃ using an electron-swarm mass
322 spectrometric technique. *International journal of mass spectrometry and ion processes* **1997**,
323 *164* (3), 207-223.

- 324 19. Bell, A.; Giles, K.; Moody, S.; Watts, P., Studies on gas-phase positive ion—
325 molecule reactions of relevance to ion mobility spectrometry The reactions of 2-methyl-2-
326 propanol (t-butyl alcohol) with protonated water clusters in an ion mobility system.
327 *International journal of mass spectrometry and ion processes* **1998**, 173 (1), 65-70.
- 328 20. Howse, D. C. Development and application of an ion mobility spectrometer-
329 quadrupole mass spectrometer instrument. PhD, University of Birmingham, 2015.
- 330 21. St J, T.; Piper, L.; Connor, J.; FitzGerald, J.; Adams, J.; Harden, C. S.; Shoff, D.;
331 Davis, D.; Ewing, R., Design aspects and operation characteristics of the lightweight
332 chemical detector. *Int. J. Ion Mobil. Spectrom.* **1998**, 1, 58-63.
- 333 22. Turner, R. B.; Taylor, S. J.; Clark, A.; Arnold, P. D. Corona discharge ion source for
334 analytical instruments. US Pat. 6 225 623, May 1 2001.
- 335 23. Atkinson, J. R.; FitzGerald, J. P.; Taylor, S. J., Vapour Generators. US 20090133469
336 A1, May 28 2009.
- 337 24. Frisch, M.; Trucks, G.; Schlegel, H.; Scuseria, G.; Robb, M.; Cheeseman, J.;
338 Scalmani, G.; Barone, V.; Mennucci, B.; Petersson, G., Gaussian 09, revision A. 1. *Gaussian*
339 *Inc., Wallingford, CT* **2009**.
- 340 25. Matias, C.; Mauracher, A.; Huber, S. E.; Denifl, S.; Limão-Vieira, P.; Scheier, P.;
341 Märk, T. D.; González-Méndez, R.; Mayhew, C. A., Dissociative electron attachment to the
342 volatile anaesthetics enflurane and isoflurane and the chlorinated ethanes pentachloroethane
343 and hexachloroethane. *International Journal of Mass Spectrometry* **2015**, 379 (0), 179-186.